A Fungal Modified Material With High Uranium (VI) Absorption Capacity And Strong Anti-Interference Ability

Ni Tan (tan_nii@163.com)
University of South China
Qiaorong Ye
University of South China
Yaqing Liu
University of South China
Yincheng Yang
University of South China
Zui Ding
University of South China
Lijie Liu
University of South China
Duoduo Wang
University of South China
Chensi Zeng
University of South China

Research Article

Keywords: polydioxyethylene ether, diamidoxime, fungal modified material, uranyl adsorption, anti-interference

Posted Date: January 6th, 2022

DOI: https://doi.org/10.21203/rs.3.rs-1157667/v1

Abstract

With polydioxyethylene ether as the bridge chain, a new fungal modified material with diamidoxime groups was prepared by a series of uncomplex synthesis reaction. The orthogonal experiment obtained its optimized adsorption conditions as follows: the initial pH value 6.5, the initial uranyl concentration 40 mg L^{-1}, the contact time 130 min, and the solid-liquid ratio 25 mg L^{-1}. The maximum adsorption capacity of target material was 446.20 mg g^{-1}, and it was much greater than that of the similar monoamidoxime material (295.48 mg g^{-1}). The linear Langmuir (R^2 = 0.9856) isotherm models and the linear pseudo-second-order kinetic model (R^2 = 0.9931) fit the experimental data of uranium (VI) adsorption better, indicating the adsorption mechanism should mainly be the monolayer adsorption and chemical process. In addition, the relevant experiments exhibited the prepared material was of the good reuse and the excellent anti-interference performance, which suggested the new acquisition should also have well-applied prospect in the future.

1. Introduction

For the treatment of heavy metal wastewater pollution, many chemical synthesized materials (Wang et al. 2016; Jin et al. 2016; Zhang et al. 2015) and natural biomass (Huo et al. 2020; Torres 2020) were used as the absorbents. It was well known that amidoxime group could be as electron donor to coordinate with uranyl ion, and the functionalized amidoxime acquisition had performed well in uranium (VI) recovery (Khouya 2010; Sun et al. 2018; Kelley et al. 2014; Vukovic et al. 2012)

According to the Hard-Soft-Acid-Base theory (Ritter 2003), UO_2^{2+} usually belongs to the hard acid and has the better coordination ability with hard base ligands, and the majority of them reported in the previous literatures were like esters containing N and O atoms with some lone pair electrons, which had good chelate properties for metal ions (Gromova et al. 2021).

Open chain polyether is a chain compound containing polyoxyethylene ether (-CH_2CH_2O-) structure unit, and it is often of the ring like structure, which property is relatively similar with macrocyclic polyester or crown ether, showing the characteristics of coordination selectivity and multi-coordination numbers. In the process of metal ion coordination, the conformation of open-chain molecule is curled, resulting in a coordination effect similar to the macroring effect (Gromova et al. 2021; Vgtle and Weber 1979; Wang and Zhuang 2020; Shi et al. 2003). Although the incorporation of heavy metal ion into the inner cavity of crown ether with strong coordination ability, the crown ether is toxic to the environment and complex in preparation with a low yield. So the material with open-chain ether structure has a certain reference significance for the treatment of wastewater containing uranyl ions.

In this paper, in order to further improve the adsorption capacity and uranium (VI) selectivity adsorption of the tested fungus *Fusarium sp*. #ZZF51 (He et al. 2019; Han et al. 2020; Liu et al. 2021), with polydioxyethylene ether as the bridge chain, the diamidoxime groups were connected to the fungal

surface, and a new modified function material was prepared. Its structure characterization, adsorption properties, reuse, and anti-interference performance were also explored in details.

2. Experiments And Methods

2.1 Reagents

3,3-iminodipropionitrile, sodium tert-butoxide (98%), hydroxylamine hydrochloride (≥98%), p-toluenesulfonyl chloride (PTSC,≥99%), pyridine, sodium hydroxide, and hydrochloric acid were supplied from McLean (Shanghai, China). 2-(2-Chloroethoxy) ethanol (98.8%) was ordered from Haohong (Shanghai, China). Uranium acetate was got from Meicheng (Shanghai, China). Methanol and ethanol were received from Yufeng (Changsha, China). Nitric acid was obtained from JianDong (Shandong, China).

Glucose was from Zhentian (Hebei, China). Peptone was obtained from Aoboxing (Beijing, China). Yeast extract was obtained from Yuanye (Shanghai, China), and sea salt was purchased from Light Industry&Salt (Hunan, China).

2.2 Synthesis of fungal modified material

By the reference(Yang et al. 2011), the original fungus mycelium for later use was obtainted. As in Fig. 1, the preparation process of fungal modified material was depicted as belows: Under nitrogen atmosphere, mycelium (1.947 g) and sodium hydroxide (1.023 g) were put into the flask containing 30 mL ethanol. After magnetic stirring at 30 ℃ for half an hour, 3 mL of 2-(2-Chloroethoxy) ethanol was added, and the temperature was adjusted to 65 ℃ and the reaction was last for 12 hours. Then the product was washed with distilled water and ethanol, filtered and dried under vacuum at 60 ℃ until no water, and intermediate (1) (1.890 g) for next step was got. At room temperature and under nitrogen environment, intermediate (1) and p-toluenesulfonyl chloride (6.441 g) were immersed in 30 mL of pyridine solution and reacted for 27 h. Then the product was filtered, washed with ethanol, dried under vacuum at 60℃, and the intermediate (2) (1.806g) was obtained. Under the same starting conditions as above, intermediate (2), 2mL of 3,3'-Iminodipropionitrile, and sodium tert-butoxide (1.796 g) were put into 40 mL of ethanol solution, and they reacted for 30 h at 55℃, then intermediate (3) (1.624 g) was got after conventional treatment. Surrounded by nitrogen, intermediate (3) and $NH_2OH{\cdot}HCl$ (2.035 g) was mixed in 40 mL methanol at 35℃ for 2.5 h. Then the pH value in solution was adjusted to 9.0, and the mixture was refluxed for 8 h at 75 ℃. The final product (1.103 g) was rinsed with deionized water and dried under vacuum at 60 ℃.

2.3 Characterization

The functional groups of materials were assessed by Fourier transform infrared spectrometer (FTIR, Nicolet IS 10, Thermo Fisher Scientific) in the wavelength range of 4000-500 cm^{-1}. The morphologies of materials were observed by scanning electron microscope (SEM, ZEISS Gemini 300, Carl Zeiss). According to Brunauer–Emmett–Teller (BET) technique and by using Brunauer Emmett Tellers instrument

(BET, ASAP 2460, Micromeritics), the surface areas of materials were got by performing nitrogen adsorption/desorption isotherms. Thermogravimetric analysis (TGA, TGA5500, TA Instruments) measured the mass change and rate of change of substances.

2.4. Absorption experiments

As in single factor adsorption experiments, the effects of pH (2.0 – 8.0), initial uranium (VI) concentrations (10 – 60 mg L^{-1}), solid-liquid ratio (50 – 400 mg L^{-1}), and contact time (30 – 240 min) on uranium (VI) adsorption capacity of the prepared materials were investigated. The pH values of solutions were adjusted by 1.0 mol L^{-1} NaOH and 1.0 mol L^{-1} HNO_3, and they were measured by pH-meter. On the basis of single factor experiments, the orthogonal experiments were designed to find the optimum adsorption condition.

To evaluate reuse performance, the fungal modified materials were added to 50 mL uranium (VI) solution for 24 h at room temperature, then they were rinsed by 1.0 mol L^{-1} HCl solution, and the concentrations of supernatants were detected to evaluate the desorption rate (Shimaa 2021; Tan et al. 2018).

In order to simulate the ionic environment of actual wastewater, Li^+ , Na^+ , K^+ , Ca^{2+} and Mg^{2+} disturbed the adsorption of uranium (VI) by materials. The initial concentration of heteroion in the solution was set at 0.5 mol L^{-1}. Under the optimal adsorption conditions, the uranyl concentration in the supernatant was measured, then the adsorption capacity was calculated.

UV spectrophotometer (Shimadzu UV-2600, Shimadzu) was used to investigate the concentration of uranium ion (Du et al. 2015).

The adsorption capacity and the percentage adsorption, were calculated by formula 1 (Peng et al. 2014) and formula 2 (Simonin 2016), respectively.

$$Q_e(mg\ g^{-1}) = \frac{(C_0 - C_e)V}{m} \quad \text{..... 1}$$

$$R\ (\%) = \frac{C_0 - C_e}{C_0} \times 100\% \quad \text{..... 2}$$

Q_e is the adsorption capacity (mg g^{-1}). R (%) is the percentage adsorption.

C_0 and C_e are respectively the initial and equilibrium uranium (VI) concentrations (mg L^{-1}).

V (L) is the volume of the solution, and m (g) is the dry mass of the modified fungus.

3. Results And Discussion

3. 1 Characterization

3.1.1 FTIR analysis

The infrared spectra of fungal primitive mycelium, intermediates(1,2,3) and fungal modified material were respectively shown in curves(a,b,c,d,e) of Fig. 2.

In the infrared spectrum curve (a), the seen bands at 3283, 2926, 1074/1032 and 1654 cm^{-1} should be respectively assigned to the stretching vibration of -OH/-NH, -CH, -C-O and –C=O/C=N groups. In curve (b), that the intensity of peaks at 1074 and 1032 cm^{-1} strengthened apparently indicated the presence of C-O-C ether chain groups. Compared with curve (b), the emergence of new peaks at 1177 and 686 cm^{-1} in curve (c) could be attributed to the stretching vibration of -S=O groups on p-toluenesulfonyl chloride and the out-of-plane bending vibration of =C-H in benzene ring, respectively. In curve (d), the vibration peak at 2175 cm^{-1} from -C≡N appeared, and the peak at 686 cm^{-1} disappeared, which explored that p-toluenesulfonyl chloride should be replaced by 3,3'-iminodipropionitrile. It could be seen in curve (e) the new characteristic telescopic vibration peak at 900 cm^{-1} attributed to -N-O appeared, and the peak areas at 1577 and 3438 cm^{-1} caused respectively by -C=N and -NH_2 vibration strengthened when compared with the other curves. All the above informations made sense that amidoxime groups had been successfully existed in the fungal modified material.

The before and after uranium (VI) adsorption were also analyzed by FTIR, as shown in the infrared spectra curves (e) and (f) of Fig. 2. After capturing U(VI), the vibration peaks of -NH_2, -C=N and -N-O respectively at 3438, 1577 and 900 cm^{-1} moved to 3425, 1559 and 925 cm^{-1}, along with the change of their intensities, which indicated that the participation of amidoxime groups in the chelation of U(VI) ions. Besides, the characteristic peak of O=U=O asymmetric stretching vibration appeared at 810 cm^{-1} (Zhang et al. 2022), demonstrating uranyl had been captured by the aim modified material.

3.1.2 SEM and BET analyses

The scanning electron microscope images of materials were shown in Fig. 3. As seen in Fig. 3(a), the surface of fungal primitive mycelium was relatively flat, that was a typical cytoderm morphology. In Fig. 3(b), it had a great change that the fungal modified material became more fluffy. When the prepared material was loaded uranyl ions, its surface seen in Fig. 3(c) became rough and uniform, and the pore size became smaller, which might be caused by the loaded-uranium on the fungal modified material surface.

BET experimental data were described in Fig. 4, the specific surface areas of fungal primitive mycelium and fungal modified material 14.8768 cm^2 g^{-1} and 22.9869 cm^2 g^{-1} were obtained, respectively. The surface area of the latter with pore size of 0-20 nm increased significantly, indicating that the pore number of the material became more and the pore surface became rougher, which was consistent with the morphology under the scanning electron microscope in Fig. 3(b). The hysteresis loop appeared in the

isotherm of BET test, indicating that multi-layer physical adsorption on the fungal modified material will not be further carried out, and then the monolayer adsorption was mainly performed.

3.1.3 TGA analysis

As shown in Fig. 5, from the temperature change of 100-200 ℃, both of two curves had the lower degree, which indicates that the fungal modified material and the loaded-uranium material had the lower pyrolysis rate and the better thermal stability. During the temperature range from 200 ℃ to 400 ℃, their weight dropped sharply and had almost the same loss rate due to the existance of a large number of ether bonds and amidoxime groups. The weight loss of the loaded-uranium material was less than the fungal modified material from 400-500 ℃, and their weight difference remained unchanged from 500 ℃ to 800 ℃, indicating that the uranyl ions loaded on the fungal modified material were highly thermally stable.

3.2 Exploration of maximum adsorption capacity

3.2.1 Single-factor experimental analysis.

Effect of solid-liquid ratio. As seen in Fig. 6(a), when the other conditions remained unchanged (T = 25 ℃, C = 20 mg L^{-1}, pH = 5.0, t = 180 min, V = 50 mL), with the increase of the amount of adsorbent, the adsorption capacity decreased, while the adsorption percentage increased, which indicated the concentration of uranyl cation in adsorption equilibrium state decreased with the increase of the amount of adsorbent, and the active sites of adsorbent related to the adsorption were also decreasing.

Effect of initial uranium(VI) concentration. Fig. 6(b) described the influence of initial uranium(VI) concentration on the adsorption ability of material when the other conditions were as follows (T = 25 ℃, S/L = 150 mg L^{-1}, pH = 5.0, t = 180 min, V = 50 mL). The adsorption capacity had an obvious maximum value when the uranium(VI) concentration changed between 35 mg L^{-1} and 45 mg L^{-1}, and after the peak, the slope of curve did not change more, which showed the amount of adsorption dose limited the number of adsorption active sites, and the adsorption reached the equilibrium state when all the active sites were fulled up by the uranyl cations. Certainly the adsorption rate decreased all the time. About 70% uranium(VI) could be removed by the material at low concentration of 10 mg L^{-1}, and the removal efficiency was just 30% at the initial uranium(VI) concentration 60 mg L^{-1}. The phenomenon explored the aim material had a good performance in the removal of low concentration uranyl ions.

Effect of pH value. To explore the effect of pH value on uranium(VI) adsorption by the fungal modified material, the absorption experiments were performed under the conditions of pH range 2.0-8.0 with these following invariant (T = 25 ℃, C = 40 mg L^{-1}, S/L = 150 mg L^{-1}, t = 180 min, V = 50 mL), and their results were shown in Fig. 6(c). As it could be seen that the effect of pH value on the adsorption capacity and the adsorption rate was almost synchronous. At the low pH, lots of H^+ and H_3O^+ acted as the competitive ions with uranium(VI) for the active adsorption sites, and the protonation of amidoxime groups also affected the adsorption course, so the data of both adsorption capacity and adsorption rate were little.

With the increasing of pH, the protonation degree of amidoxime groups gradually decreased, and the uranyl adsorption capacity reached the maximum (105 mg g^{-1}) when the pH value was 6.0. At the high pH, the negatively charged uranyl lions [$UO_2(OH)_3^-$, $(UO_2)_3(OH)_7^-$, $UO_2(OH)_2$] were the dominated species, and the colloidal precipitates formed by the hydrolysis of uranium ions (Cheng et al. 2021), resulting in the decrease of adsorption capacity and adsorption rate. From the above, it could be known that pH played an important role in the uranium(VI) removal process.

Effect of contact time. As shown in Fig. 6(d), the change of adsorption percentage was consistent with that of adsorption capacity. Under a certain conditions (T = 25 ℃, C = 40 mg L^{-1}, S/L = 150 mg L^{-1}, pH = 5.0, V = 50 mL), both the adsorption capacity and the adsorption rate increased with prolonging the contact time in the initial stage of adsorption, then the material tended to reach the adsorption equilibrium. When continuing to increase the contact time, the slopes of curves decreased a little, indicating some of uranyl ions on the surface of adsorption material were free and movable, which could affect the adsorption data. So the physical adsorption partly existed on the material surface, certainly the chemical adsorption should play a important role in the whole adsorption course.

3.2.2 Orthogonal experimental design and analysis

Based on the above single factor experiments, the orthogonal design L9(3^4) and its related experiments were carried out, and the specific implemented scheme was list in Tab. 1 and Tab. 2. By comparing the experimental data of *K* and *R*, the optimum adsorption conditions were finally obtained as follows: the initial uranium (VI) concentration 40 mg L^{-1}, the solid-liquid ratio 25 mg L^{-1}, the initial pH 6.5, and the contact time 130 min, and the corresponding maximum adsorption capacity was 446.20 mg g^{-1}.

Thanks to the growth of polyether chain in the fungal modified material, the adsorption capacity of uranium (VI) had been greatly improved, because the adsorption capacity of the prepared material containing two basic polyether in this paper was nearly 70 mg g^{-1} more than that of the single basis polyether material synthesized by Dianxiong He in our lab (He et al. 2019). In addition, the number of amidoxime groups at the end of modified material could also obviously affect the adsorption capacity of uranyl ions, since the adsorption capacities of target material with diamidoxime groups and the fungal-modified material containing the monoamidoxime terminal open-chain polyether by Yaqing Liu (Liu et al. 2021) were respectively 446.20 mg g^{-1} and 295.48 mg g^{-1} and the adsorption capacity of tri-amidoxime modified marine fungus material (ZZF51-GPTS-EDA-AM/ZGEA) with the single basis polyether prepared by Jingwen Han (Han et al. 2020) attained 584.60 mg g^{-1}, which showed that the amidoxime groups in material played an obvious role in the adsorption of uranium (VI).

Tab.1 Orthogonal experiment parameters and levels

Parameters	1	2	3
solid-liquid ratio (mg L^{-1})	25	50	75
U(VI) concentration (mg L^{-1})	35	40	45
initial pH	5.5	6.0	6.5
contact time (min)	110	120	130

Tab.2 The data of orthogonal experiments

Testing number	Parameters				Adsorption Capacity(mg g^{-1})
	U(VI) concentration (mg L^{-1})	Solid-liquid ratio (mg L^{-1})	Initial pH	Contact time (min)	
1	35	25	5.5	110	272.10
2	35	50	6.0	120	253.24
3	35	75	6.5	130	203.18
4	40	25	6.0	130	446.20
5	40	50	6.5	110	374.40
6	40	75	5.5	120	142.27
7	45	25	6.5	120	343.62
8	45	50	5.5	130	197.03
9	45	75	6.0	110	163.07
K_1	242.84	353.97	203.80	269.86	
K_2	320.96	274.89	287.50	246.38	
K_3	234.57	169.51	307.07	282.14	
R	86.39	184.46	103.27	35.76	

3.3 Reusability analysis

The reusability is essential to evaluate the applicability of adsorbent. Fig. 7 displayed the reusability data of fungal modified material for five adsorption-desorption cycles. With the increasing number of adsorption-desorption cycle, the adsorption capacity gradually decreased and finally reached 84.25% of

that of material at the first time after five cycles. Of course, the ability to absorb uranium (VI) for the material held up remarkably well, and the decrease of adsorption capacity might be due to the weakening of mechanical strength in the material, which was repeated washing by the eluent HCl.

3.4 Anti-interference research

As shown in Fig. 8, in the case of interference cations (Li^+, Na^+, K^+, Ca^{2+}, Mg^{2+}) in the uranium (VI) solution, the adsorption capacity of the material could still reach about 440 mg g^{-1}, which was slightly less than that under the optimal adsorption conditions. This revealed that the presence of various cations had no obvious effect on the uranium (VI) removal performance of fungal modified material. Further more, the above data could also exhibit the selectivity adsorption to uranium (VI) for material in the environmental wastewater containing multiple cations, and this would be of great value in the future practical application.

3.5 Adsorption isotherm

To determine the absorption behavior and the feature of target material, nowadays, Langmuir, Freundlich, and Temkin models are widely accepted and applied in the adsorption isotherm study (Peng et al. 2014). The corresponding thermodynamic parameters were listed in Tab. 3. The data showed the linear Langmuir isotherm model (R^2 = 0.9856 and RMSE = 0.0027) could better describe the adsorption process. In the ideal state, Langmuir isothermal model denoted the monolayer adsorption process, and the adsorbed particles were completely independent rather than interactive. So, it was inferred that the adsorption of uranyl in this research mainly occurred via the monolayer manner on the homogeneous surface, and this was highly agreed with the previous result of BET in 3.1.2.

Tab. 3 The parameters of isotherm adsorption models

Models							
Langmuir			Freundlich			Temkin	
Parameters	Linear	Nonlinear	Parameters	Linear	Nonliner	Parameters	Values
Q_e(mg g^{-1})	141.0400	144.8400	K_F	32.0000	143.0100	A	1.4875
b_L(L g^{-1})	1.0001	0.1375	n	2.5790	1.2887	B	31.0996
R^2	0.9856	0.9576	R^2	0.9408	0.9613	R^2	0.9413
RSEM	0.0027	66.7900	RSEM	63.5300	60.8900	RSEM	64.1600

3.6 Adsorption kinetics

In order to study the kinetic behavior of uranium (VI) adsorption, the related parameters were calculated by drawing pseudo first-order, pseudo second-order and elovich kinetic models (Simonin 2016; Lin and Wang 2009). Two error analysis methods of the linear and the nonlinear regression were selected by comparing their determination coefficient (R^2) and the residual root mean square error (RMSE). The higher the R^2 and the smaller the RMSE, indicating the higher the fitting degree with the data (Monika et al 2019).

The parameters of kinetic models were showed in Tab. 4. As it was seen, R^2 (0.9931) and RMSE value (0.0059) of the pseudo-second-order kinetic linear model were respectively the maximum and the minimum, which explored it was more consistent with the experimental data. Generally speaking, The pseudo-second-order kinetics model was based on the chemical adsorption, such as the electron transfer or the electron sharing between the adsorbent and uranyl ions. So, it was inferred that the rate limiting step of uranium (VI) adsorption in this paper should mainly be the chemical reaction such as complexation or chelation, consistent with the result in the previous contact time experiments.

Tab. 4 The parameters of kinetics adsorption models

Models							
Pseudo-first-order			Pseudo-second-order			Elovich	
Parameters	Linear	Nonlinear	Parameters	Linear	Nonlinear	Parameters	Values
K_1	0.0094	0.03479	K_2	0.0010	17.2800	α	48.4000
Q_e(mg g^{-1})	25.7900	81.0512	Q_e(mg g^{-1})	85.8400	89.3500	β	0.0805
R^2	0.6438	0.8791	R^2	0.9931	0.8748	R^2	0.7943
RMSE	0.3671	13.5678	RMSE	0.0059	14.0500	RMSE	2.5813

4.conclusion

By the above characterization data of FITR, SEM, TGA, and BET, a new modified fungal material characterized with polydioxyethylene ether as the bridge chain and diamidoxime as the terminal groups was proved synthesized successfully. Through the single factor and orthogonal experiments, the best adsorption conditions (initial uranium (VI) concentration 40 mg L^{-1}, solid-liquid ratio 25 mg L^{-1}, initial pH 6.5, and contact time 130 min) were found out, and the maximum adsorption capacity of the target material was obtained 446.20 mg g^{-1}, which was 29 times that of the native fungus (15.46 mg g^{-1}) (Yang et al. 2011), and almost twice as much as that of the similar monoamidoxime material (295.48 mg g^{-1}) (Liu et al. 2021). In the anti-interference experiment, it is speculated that the acquisition had the strong anti-interference performance to the other ions such as Li^+, Na^+, K^+, Ca^{2+}, and Mg^{2+}, which could well interpreted the new material was of the better uranyl selective adsorption. Combined with the excellent

reusability, the prepared material should have a certain application value in the treatment of wastewater containing uranium (VI).

Declarations

Ethical Approval and Consent to Participate

Not applicable.

Consent to Publish

Not applicable

Availability of data and materials

All data and materials generated or analyzed during this study are included in this published article and its supplementary information.

Funding

This work was financially supported by the Natural Science Foundation of Hunan Province (No.2020JJ4520), and the Research Learning and Innovative Experimental Program of Hunan/University South of China (X2019070, S202110555135)

Competing interests

The authors declare no competing interests

Authors Contributions

Ni Tan contributed to the study conception and design. Material preparation, experiments, data collection and analysis were performed by Qiaorong Ye and Yaqing Liu. The first draft of the manuscript was written by Qiaorong Ye and Yaqing Liu. Yincheng Yang, Zui Ding, Lijie Liu, Duoduo Wang and Chensi Zeng commented on previous versions of the manuscript. All authors read and approved the final manuscript.

References

1. Cheng YX, Li FZ, Liu N, Lan T, Yang YY, Zhang T, Liao JL, Qing RW (2021) A novel freeze-dried natural microalga powder for highly efficient removal of uranium from wastewater. Chemosphere 282:131084
2. Du L, Li YX, Ma X, Liu YG (2015) Spectrophotometric determination of trace uranium with arsenazo â…¢. Metallurgical Analysis 35:68–71. (in Chinese)

3. Gromova VF, Ikima MI, Gerasimova GN, Trakhtenberg LI (2021) Crown ethers: selective sorbents of radioactive and heavy metals. Russian Journal of Physical Chemistry B 15:140–152
4. Han JW, Hu L, He LQ, Ji K, Liu YQ, Chen C, Luo XM, Tan N (2020) Preparation and uranium (VI) biosorption for tri-amidoxime modified marine fungus material. Environ Sci Pollut Res 27:37313–37323
5. He DX, Tan N, Luo XM, Yang XC, Ji K, Han JW, Chen C, Liu YQ (2019) Preparation uranium (VI) absorption and reuseability of marine fungus mycelium modified by the bis-amidoxime-based groups. Radiochimica Acta 108:37–49
6. Huo ZP, Zhao S, Yi JX, Zhang H, Li JX (2020) Biomass-based cellulose functionalized by phosphonic acid with high selectivity and capacity for capturing U(VI) in aqueous solution. Applied Sciences 10:5455
7. Jin C, Hu JT, Wang JQ, Xie CY, Wu GZ (2016) An amidoximated-UHMEPE fiber for selective and high efficient removal of uranyl and thorium from acid aqueous solution. Advances in Chemical Engineering & Science 7:45–59
8. Kelley SP, Barber PS, Mullins PHK, Rogers RD (2014) Structural clues to UO22+/VO2+ competition in seawater extraction using amidoxime-based extractants. Chemical Communications 50:12504–12507
9. Khouya EH, Legrouri K, Fakhi S, Hannache H (2010) Adsorption of uranium and thorium on new adsorbent prepared from moroccan oil shale impregnated with phosphoric acid. Nature Precedings 5:5098
10. Lin JX, Wang L (2009) Comparison between linear and non-linear forms of pseudo-first-order and pseudo-second-order adsorption kinetic models for the removal of methylene blue by activated carbon. Frontiers of Environmental Science and Engineering in China 3:320–324
11. Liu YQ, Chen C, He LQ, Hu L, Ding Z, Liao S, Tan N (2021) Preparation of a fungal-modified material linked by the monoamidoxime terminal open-chain polyether and its uranyl adsorption. Ind Eng Chem Res 60:4705–4713
12. Monika Chaudhary A, Lovjeet Singh B, Pawan Rekha C, Vimal Chandra Srivastava B, Paritosh Mohanty A (2019) Adsorption of uranium from aqueous solution as well as seawater conditions by nitrogen-enriched nanoporous polytriazine. Chem Eng J 378:122236
13. Peng S, Meng HC, Ouyang Y, Chang J (2014) Nanoporous magnetic cellulose–chitosan composite microspheres: preparation, characterization, and application for Cu(II) adsorption. Industrial & Engineering Chemistry Research 53:2106–2113
14. Ritter S (2003) Hard and soft acids and bases. Chem Eng News 81:0–50
15. Shi Y, Guo F, Wang YH (2003) Open chain crown ether. Journal of Tianshui Normal University 23:33–36. (in Chinese).
16. Shimaa SH (2021) New studies of uranium biosorption by extracellular polymeric substances (EPSs) of aspergillus clavatus, using isotherms, thermodynamics and kinetics. Int J Environ Stud 78:228–246

17. Simonin JP (2016) On the comparison of pseudo-first order and pseudo-second order rate laws in the modeling of adsorption kinetics. Chemical Engineering Journal 300:254–263
18. Sun Q, Aguila B, Earl LD, Abney CW, Wojtas L, Thallapally PK, Ma SQ (2018) Covalent organic frameworks as a decorating platform for utilization and affinity enhancement of chelating sites for radionuclide sequestration. Adv Mater 30:1705479
19. Tan Y, Li L, Zhang H, Ding DX, Dai ZG, Xue JH, Liu JQ, Hu NY, Wang YD (2018) Adsorption and recovery of U(VI) from actual acid radioactive wastewater with low uranium concentration using thioacetamide modified activated carbon from liquorice residue. J Radioanal Nucl Chem 317:811–824
20. Torres E (2020) Biosorption: A review of the latest advances. Processes 8:1584
21. Vgtle F, Weber E (1979) Multidentate acyclic neutral ligands and their complexation. Angewandte Chemie International Edition in English 18:753–776
22. Vukovic S, Watson LA, Kang SO, Custelcean R, Hay BP (2012) How amidoximate binds the uranyl cation. Inorganic Chemistry 51:3855–3859
23. Wang FH, Li HP, Liu Q, Li ZS, Li RM, Zhang HS, Liu HL, Emelchenko GA, Wang J (2016) A graphene oxide/amidoxime hydrogel for enhanced uranium capture. Sci Rep 6:19367
24. Wang JL, Zhuang ST (2020) Cesium separation from radioactive waste by extraction and adsorption based on crown ethers and calixarenes. Nuclear Engineering and Technology 52:328–336
25. Yang HB, Tan N, Zhang HP, Deng CA, Sun M, Lin YC, She ZG (2011) Adsorption of uranium(â…¥) by the mangrove endophytic fungus fusarium sp. #ZZF51 from the south china sea. Journal of Nuclear and Radiochemistry 33:358–362
26. Zhang G, Fan HM, Zhou RY, Yin WY, Wang RB, Yang M, Xue ZY, Yang YS, Yu JX (2022) Decorating UiO-66-NH2 crystals on recyclable fiber bearing polyamine and amidoxime bifunctional groups via cross-linking method with good stability for highly efficient capture of U(VI) from aqueous solution. J Hazard Mater 424:127273
27. Zhang JY, Zhang N, Zhang LJ, Fang YZ, Deng W, Yu M, Wang ZQ, Li L, Liu XY, Li JY (2015) Adsorption of uranyl ions on amine-functionalization of MIL-101(Cr) nanoparticles by a facile coordination-based post-synthetic strategy and x-ray absorption spectroscopy studies. Sci Rep 5:13514

Figures

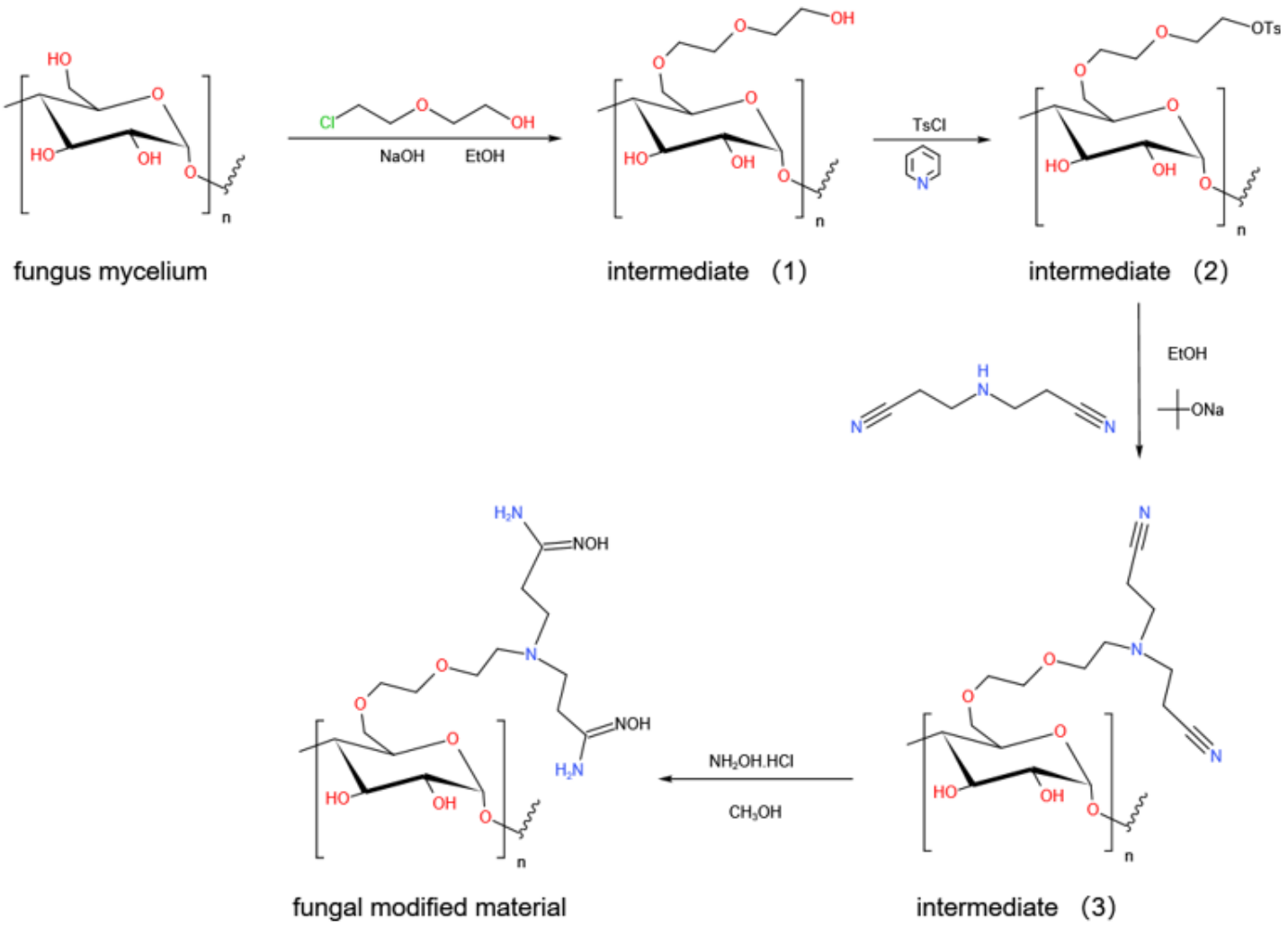

Figure 1

The preparation process of fungal modified material

Figure 2

FTIR spectra of materials. (**a**) fungal primitive mycelium. (**b**) intermediate (1). (**c**) intermediate (2). (**d**) intermediate (3). (**e**) fungal modified material. (**f**) fungal modified material after adsorption

Figure 3

SEM images. (**a**) fungal primitive mycelium. (**b**) fungal modified material. (**c**) loaded-uranium material

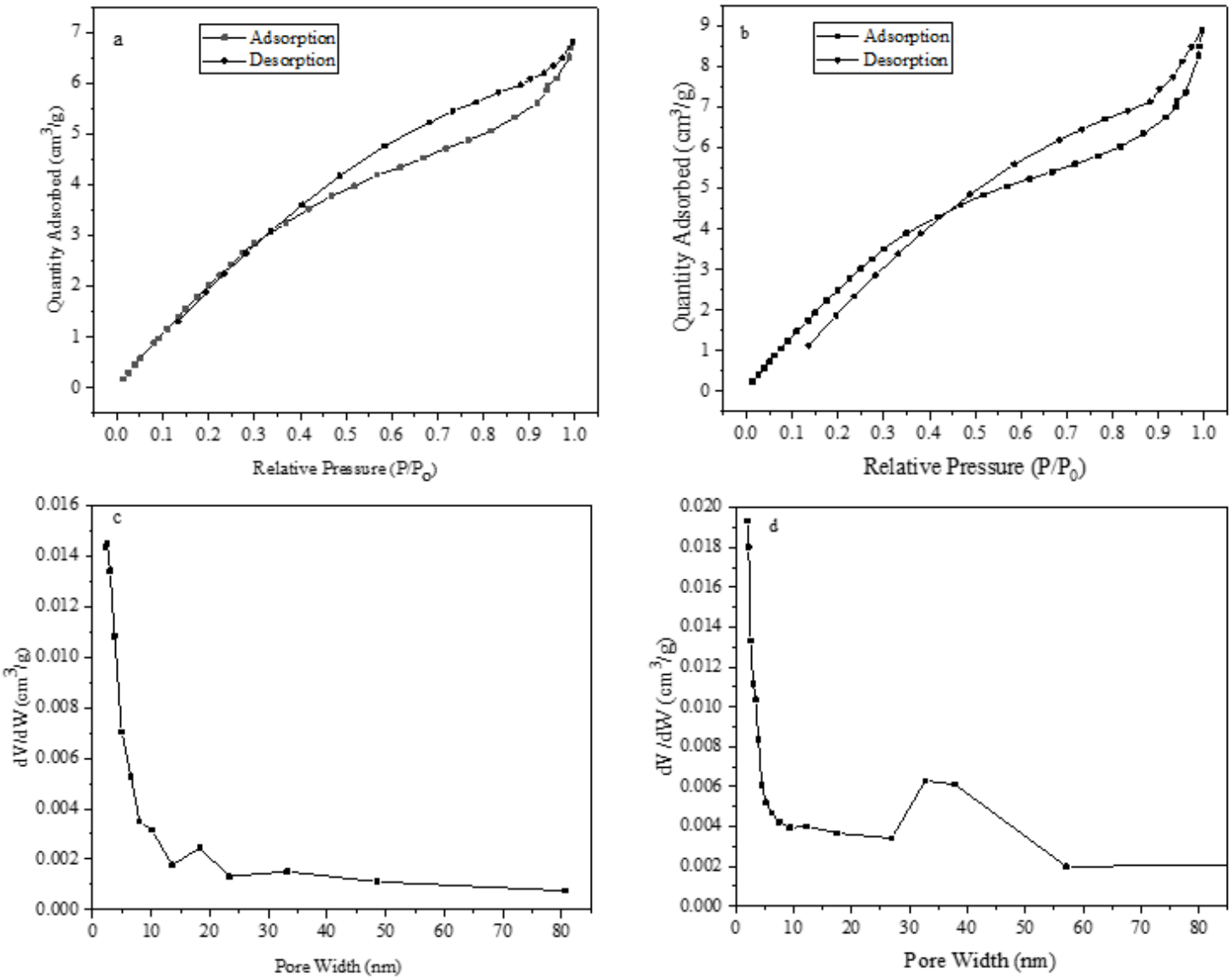

Figure 4

N_2 adsorption-desorption isotherms. (**a**) fungal primitive mycelium. (**b**) fungal modified material. Distribution characteristics of pore size. (**c**) fungal primitive mycelium. (**d**) fungal modified material

Figure 5

TGA curves of the fungal modified material and the loaded-uranium material

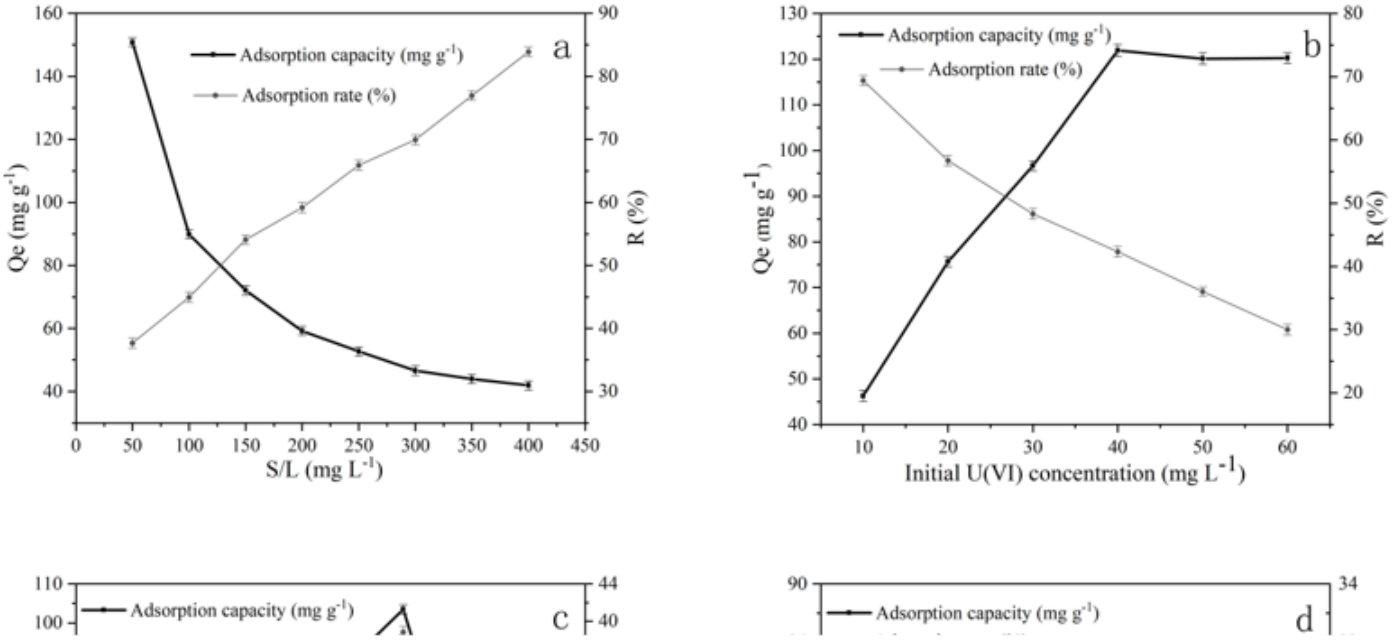

Figure 6

Effect on the U(VI) adsorption capacity and the adsorption rate. (**a**) solid-liquid ratio. (**b**) initial U(VI) concentration. (**c**) pH value. (**d**) contact time

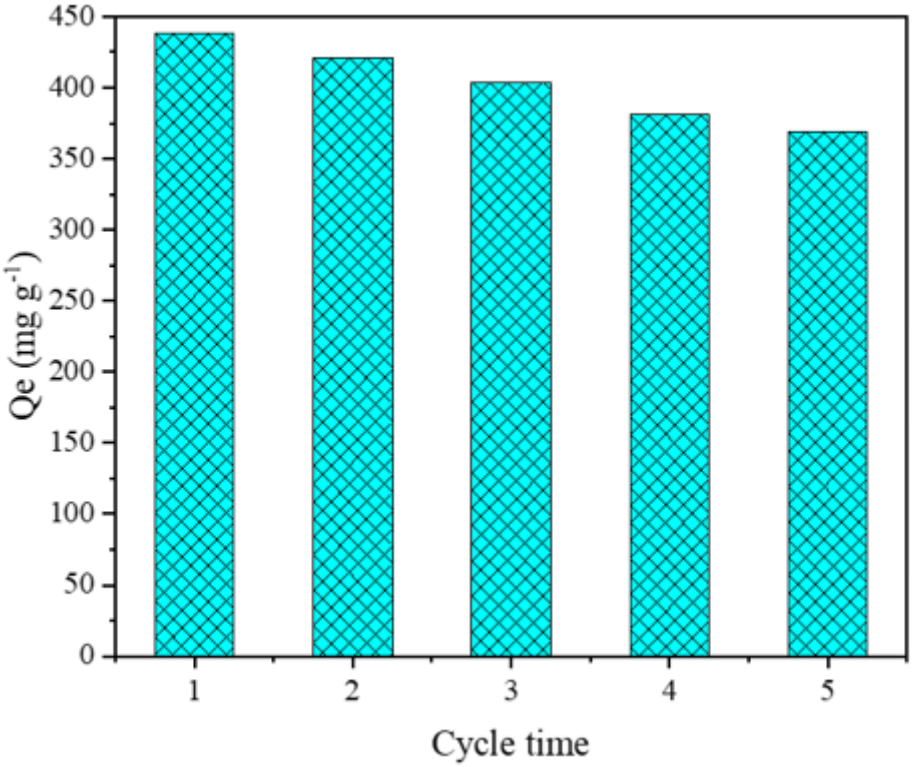

Figure 7

Adsorption-desorption cycle data of material

Figure 8

Anti-interference ability of fungus modified material in coexisting ions environment

Supplementary Files

This is a list of supplementary files associated with this preprint. Click to download.

- SupplementaryInformation.pdf